

# Pressure-pulsed chemical vapour infiltration of SiC into two-dimensional-Tyranno/SiC particulate preforms from $\text{SiCl}_4\text{-CH}_4\text{-H}_2$

YOSHIMI OHZAWA, MITSUTAKA TAKAHASHI, KOHZO SUGIYAMA  
*Department of Applied Chemistry, Aichi Institute of Technology, Yachigusa 1247,  
 Yakusa-cho, Toyota 470-03, Japan*

SiC was infiltrated in two-dimensionally woven Tyranno/SiC particulate preforms from  $\text{SiCl}_4\text{-CH}_4\text{-H}_2$  using pressure-pulsed chemical vapour infiltration (PCVI) in the temperature range 1348–1423 K. Above 1373 K, only  $\beta$ -SiC was deposited, whereas, at 1348 K, Si codeposition was found. At 1423 K, a macrosurface film was formed in the early stage of PCVI. At 1373 K, residual porosity decreased from 30% to 7.5% irrespective of the sample size. Three point flexural strength increased with decreasing residual porosity and increasing fibre volume fraction in the sample. Flexural strength of the sample having 48% fibre volume fraction reached about 325 MPa after  $5 \times 10^4$  pulses of CVI at 1373 K. Inter-laminar shear strength of the sample obtained at 1373 K reached 40 MPa at  $7 \times 10^4$  pulses.

## 1. Introduction

Among the production processes of ceramic composites, such as a fibre-reinforced SiC, chemical vapour infiltration (CVI) has the advantage of forming a product which has the same shape and size as the preform. Among the CVI processes, three methods have been developed; isothermal and isobaric CVI (ICVI), forced CVI (FCVI), and pressure-pulsed CVI (PCVI). ICVI has the characteristic of producing a near-net-shape product, however, it needs a long operation time [1–3]. FCVI, which uses steep gradients of pressure and temperature, has the advantage of a short operation time (20–40 h), however, it has a limitation on the shape of the preforms [4–6]. PCVI consists of sequential steps of evacuation of the reaction vessel, instantaneous introduction of the source gas, and holding conditions to allow deposition [7–12]. PCVI allows the production of near-net-shape products with an operation time similar to that reported for FCVI, i.e. 40–60 h for  $10^5$  pulses.

For CVI of a SiC-matrix, methyltrichlorosilane (MTS)- $\text{H}_2$  and  $\text{SiCl}_4\text{-CH}_4\text{-H}_2$  can be used as the source gases. The former system has been used most frequently, however, this source is expensive compared with  $\text{SiCl}_4\text{-CH}_4\text{-H}_2$ . Furthermore, Si can codeposit with SiC under low temperature conditions i.e. below 1273 K [13]. Codeposition of Si causes a reduction in the strength of deposits at high temperature. Elevation of the temperature above 1373 K prevents SiC–Si codeposition, however, the deposition rate of SiC from the system MTS- $\text{H}_2$  accelerates above 1173 K, therefore, films on macrosurfaces are easily formed. One of the authors of this paper has already investigated the PCVI process of transforming

SiC into porous carbon from  $\text{SiCl}_4\text{-CH}_4\text{-H}_2$  and reported that SiC single phase was obtained above 1373 K and that SiC matrix could be infiltrated into 0.2–0.5  $\mu\text{m}$  pores in porous carbon at 1373 K [14]. In the present study, we investigated the PCVI of SiC into two-dimensional-Tyranno (2D-Tyranno) fibre/SiC particulate preforms from the gas system  $\text{SiCl}_4\text{-CH}_4\text{-H}_2$ , and evaluated the flexural strength and inter-laminar shear strength (ILSS).

## 2. Experimental procedure

2-D-Tyranno/SiC particulate preforms were prepared according to the following multiple step procedure. In a first step, two-dimensional woven Tyranno cloths (Ube Industry Ltd.) were coated on both sides with SiC particles (Showa Denko Co.; average particle sizes 5  $\mu\text{m}$ ) using phenolic resin (Fenolite #3000, Dai-Nihon Ink Co.) as a binder. In a second step, two sheets of cloth were stacked, pressed and dried at room temperature for 24 h. In a third step, the stacked cloths were baked in Ar at 1273 K for 4 h, and finally, were cut to the desired size. Three type of preforms having different sizes and fibre volume fractions were prepared. Specific properties of these preforms are shown in Table I. The composition and properties of Tyranno fibre are as follows: composition (wt %) Si, 48–57; C, 30–32; Ti, 2.0; O, 12–18; number of filaments per yarn, 1600; diameter of filament, 8.5  $\mu\text{m}$ ; density, 2.3  $\text{g cm}^{-3}$ ; and tensile strength, 3.0–3.6 GPa.

The apparatus for the PCVI of SiC is shown in Fig. 1.  $\text{H}_2$  saturated with  $\text{SiCl}_4$  was held in a reservoir together with  $\text{CH}_4$ . The gas mixture in the reservoir

TABLE I Specific properties of preforms

Type	Dimension (mm) (length) × (width) × (thickness)	Porosity (%)	Fibre volume fraction (%)
A	20 × 9 × 1.8	30	29
B	35 × 9 × 2.1	30	25
C	35 × 8 × 1.1	30	48

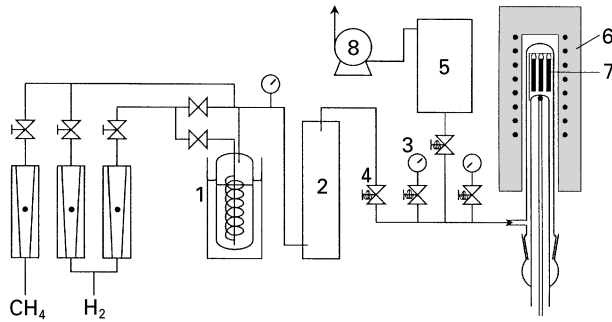


Figure 1 Apparatus for pressure-pulsed CVD of SiC. 1, SiCl<sub>4</sub> saturator; 2, reservoir; 3, pressure gauge; 4, electromagnetic valve; 5, vacuum tank; 6, furnace; 7, preform; 8, vacuum pump.

was introduced instantaneously into a reaction vessel up to 0.1 MPa, and held for 1 s to allow SiC deposition (holding time), and evacuated to below 0.7 KPa. The evacuation time being 1 s, therefore, one pulse required 2.0 s, and 10<sup>4</sup> pulses about 5.6 h. The concentrations of SiCl<sub>4</sub> and CH<sub>4</sub> were kept at 4% (SiCl<sub>4</sub>/CH<sub>4</sub> = 1). Three preforms were hung at the top of the reaction vessel.

The filling ratio of SiC infiltrated into the preform is defined as follows:

$$(\text{Filling ratio, \%}) = 100 \times (\text{Volume of infiltrated SiC} / \text{Volume of initial pore of preform})$$

The volume of infiltrated SiC was estimated roughly from the weight increase after subtraction of the weight of the macrosurface film, the thickness of which was measured on a scanning electron micrograph, and assuming the density of SiC to be 3.12 g cm<sup>-3</sup>.

The flexural strength ( $F_f$ ) was measured by the three-point method at room temperature using the following equation

$$F_f = 3 PL / 2 b d^2$$

where  $P$  = braking load,  $L$  = support span length,  $b$  = width of sample and  $d$  = thickness of sample. ILSS ( $F_I$ ) was measured by the short beam bending method at room temperature using the following equation (ASTM standard D-2344)

$$F_I = 3 P / 4 b d$$

During ILSS measurements, the  $L/d$  ratio was kept constant and equal to 4, according to the ASTM recommendation.

### 3. Results and discussion

#### 3.1. Effect of temperature and number of pulses on filling ratio and flexural strength

Fig. 2 shows the relation between the number of pulses and the filling ratio of SiC infiltrated into an A-type preform for different temperatures. At 1373 K, the filling ratio increases with number of pulses up to 7 × 10<sup>4</sup> pulses, after which it saturates at 75%, which is equivalent to a residual porosity of 7.5%. At 1423 K, the filling ratio saturates at 30% above 3 × 10<sup>4</sup> pulses, whereas, at 1348 K, the filling ratio is still increasing even after 7 × 10<sup>4</sup> pulses. At 1423 K, the deposition rate of SiC is so high that the films are easily formed on a macrosurface at an early stage, which stops the in-depth gas penetration into the preforms, therefore, the CVD temperature has to be reduced below 1373 K to attain a high filling ratio in the present system. In Fig. 3, XRD patterns from the external surface of the samples obtained at various temperatures are shown. Sharp peaks of α-SiC and β-SiC are from SiC particles in the original preforms, and the broad peaks are from the deposited matrix. All the broad peaks recorded at 1373 K and 1423 K are assigned to β-SiC, however, at 1348 K, a broad peak due to Si is also observed. Sharp peaks of SiC particles weaken or disappear for the samples processed above 1373 K. This indicates that thick films have formed on the external surface of the preforms. From the results of Figs 2 and 3, the most favourable temperature to obtain a high filling ratio of SiC without Si codeposition is considered to be 1373 K.

Scanning electron microscope (SEM) images of polished cross-sections of the samples after 9 × 10<sup>4</sup> pulses at 1373 K are shown in Fig. 4. The numbered areas in the low-magnification micrograph (left-top) are shown in the high-magnification micrographs again. Position 1 shows the interface area between the yarn of Tyranno fibres parallel to the long edge of the sample and those perpendicular to it. Position 2 shows the interface between the layer of SiC particles and the

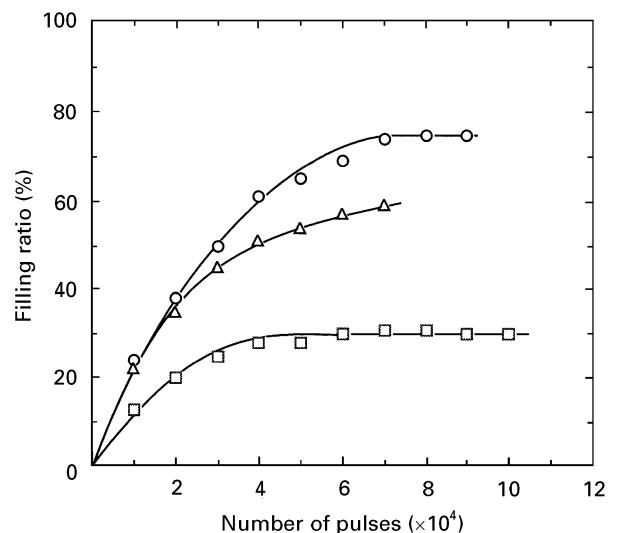


Figure 2 Relation between number of pulses and filling ratio of SiC infiltrated into an A-type preform at various temperatures; ○ 1373 K, △ 1348 K, □ 1423 K.

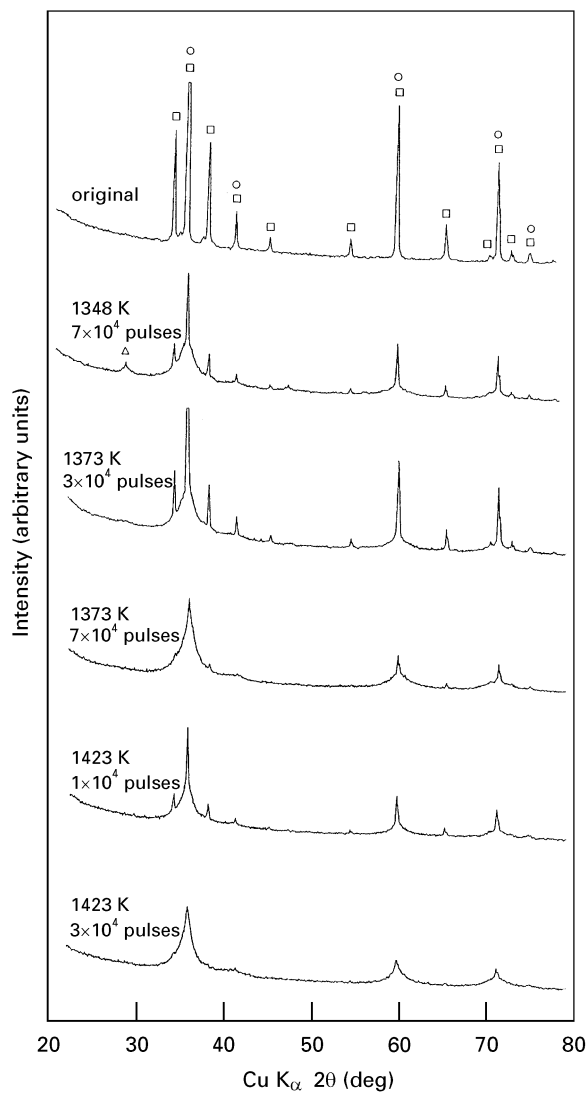


Figure 3 XRD patterns of the external surface of the A-type original preform and related infiltrated samples; ○ β-SiC, □ α-SiC, △ Si.

Tyranno fibre layer. Position 3 shows the image of the yarn parallel to the long edge of the sample at a still larger magnification. The low-magnification micrograph (left-top) shows that the composite is composed of stacks of Tyranno cloth layer and layers of SiC particles. From the micrograph of position 1, it is found that adhesion between two right-angled yarns is good. Layers of SiC particles and Tyranno layers also adhere tightly (position 2). In the micrograph of position 3, residual pores with a size below  $7\ \mu\text{m}$  are observed between the fibres.

The dependence of the flexural strength on number of pulses is shown in Fig. 5. The strength of the sample obtained at 1373 K increases with number of pulses, and reaches about 270 MPa for  $7 \times 10^4$  pulses, this strength value being about 8 to 9 times that of the original preforms. On the other hand, the strength of the sample obtained at 1423 K becomes constant and equal to 100 MPa above  $3 \times 10^4$  pulses. The low strength of the sample obtained at 1423 K results from the low filling ratio, as shown in Fig. 2.

### 3.2. Effect of sample size and fibre volume fraction on filling ratio and flexural strength

The relation between the number of pulses and the filling ratio of SiC infiltrated into B-type and C-type preforms at 1373 K is shown in Fig. 6. The filling ratio for B-type and C-type preforms increases up to  $6 \times 10^4$  and  $5 \times 10^4$  pulses, after which it levels at 79% and 73%, respectively. Saturated values for B-type and C-type preforms are close, although the C-type preform is thinner than the B-type preform. These saturated values are also close to that of the A-type preform (Fig. 2), which is shorter in length than the B-type and C-type preforms.

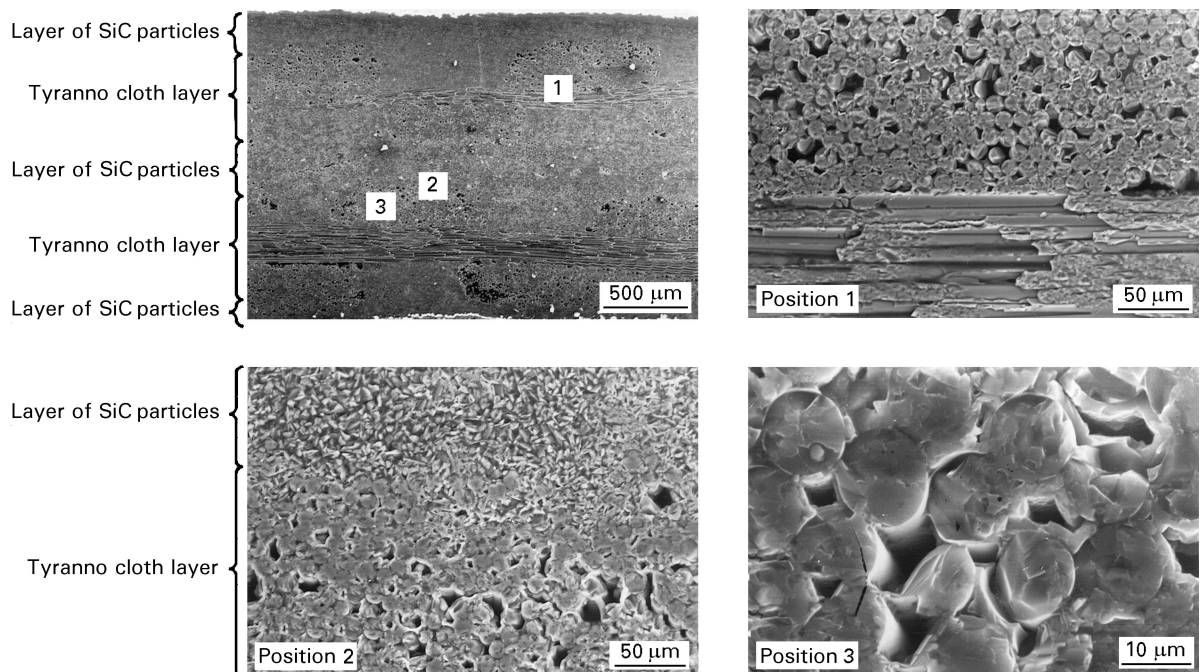


Figure 4 SEM images of the polished cross-section of the sample obtained at 1373 K after 90 000 pulses, from a preform of type-A. The numbered positions areas in the low-magnification micrograph (left-top) are shown in the high-magnification micrographs again.

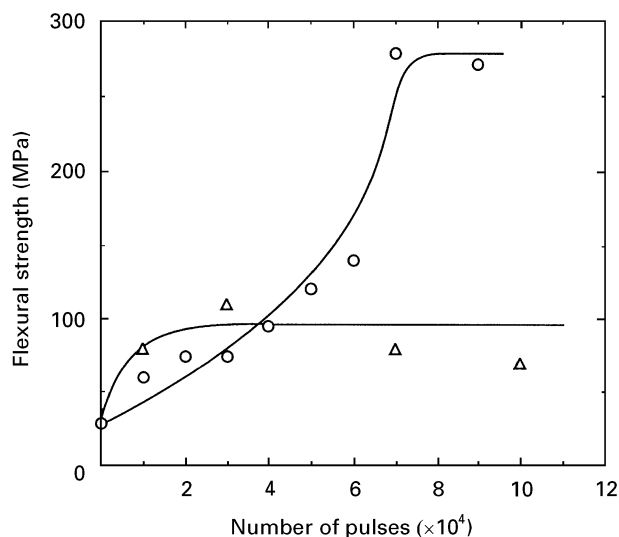


Figure 5 Dependence of flexural strength on number of pulses; preform, type-A.  $L/d$  ratio for bending test, 8.3, where  $L$ : support span length,  $d$ : thickness of sample;  $\circ$  1373 K,  $\Delta$  1423 K.

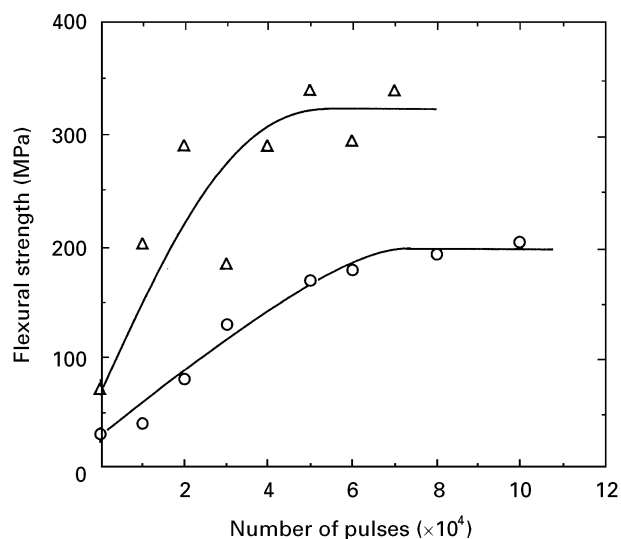


Figure 7 Dependence of flexural strength on number of pulses; CVI temperature, 1327 K.  $L/d$  ratio: B-type preform ( $\circ$ ), 14.3; C-type preform ( $\Delta$ ), 27.3.

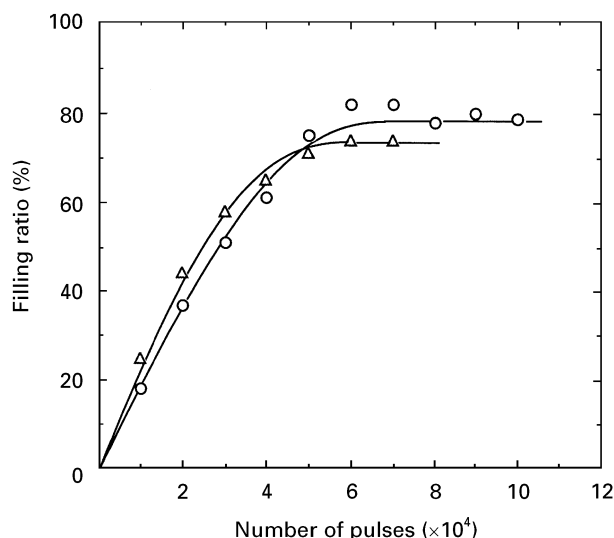


Figure 6 Relation between number of pulses and filling ratio of SiC infiltrated at 1373 K,  $\circ$  type-B,  $\Delta$  type-C.

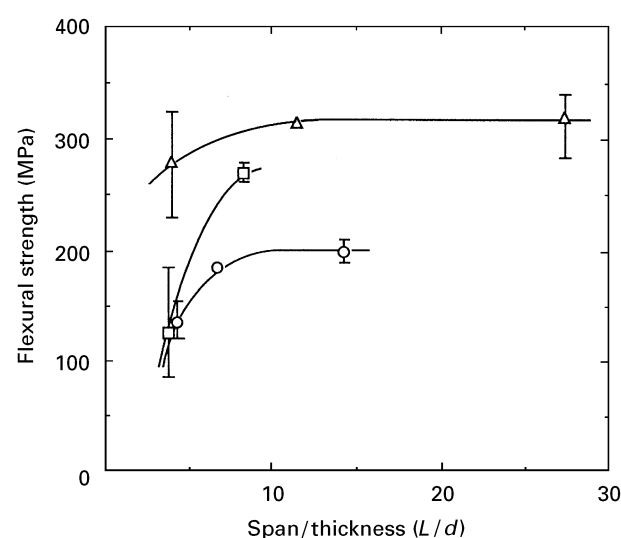


Figure 8 Relation between flexural strength and  $L/d$  ratio for the bending test; CVI temperature, 1373 K. Number of pulses: type-A ( $\square$ ),  $7 \times 10^4$ – $9 \times 10^4$ ; type-B ( $\circ$ ),  $6 \times 10^4$ – $1 \times 10^5$ ; type-C ( $\Delta$ ),  $4 \times 10^4$ – $7 \times 10^4$ . (Flexural strength saturates in the range of number of pulses mentioned above.)

The dependence of the flexural strength of the samples obtained at 1327 K using B-type and C-type preforms on the number of pulses is shown in Fig. 7. Reflecting the saturation of filling ratio (Fig. 6) above  $6 \times 10^4$  pulses in type-B and  $5 \times 10^4$  in type-C preforms, flexural strength also saturates at about 200 MPa, in type-B, and 325 MPa, in type-C preforms. The saturated strength value of type-C composites, is about 1.7 times greater than that of type-B composites, although the filling ratio is similar in both samples. The type-B and type-C samples are different in  $L/d$  ratio from the 3-point bending test (type-B, 14.3; type-C, 27.3) and in fibre volume fraction (type-B, 25%; type-C, 48%), where  $L$  is span length and  $d$  is thickness of sample. In Fig. 8, the relation between the flexural strength and the  $L/d$  ratio is shown. The flexural strength increases with the  $L/d$  ratio when  $L/d$  is below about 8, however, it becomes constant above  $L/d = 8$ . As the  $L/d$  ratio of the sample shown in Fig. 7

is above 8, the strength values in Fig. 7 are independent of the  $L/d$  ratio. On the other hand, the dependence of the flexural strength on the fibre volume fraction is shown in Fig. 9. The flexural strength and the fibre volume fraction are roughly linearly interdependent.

### 3.3. Rupture and fracture modes on bending

In the bending test, the bending moment causes bending rupture, and the shear force causes inter-laminar shear fracture. The bending moment increases with increasing span length, whereas the shear force does not depend on the span length. Therefore, for the sample in which the inter-laminar shear strength (ILSS) is low, the inter-laminar shear fracture occurs

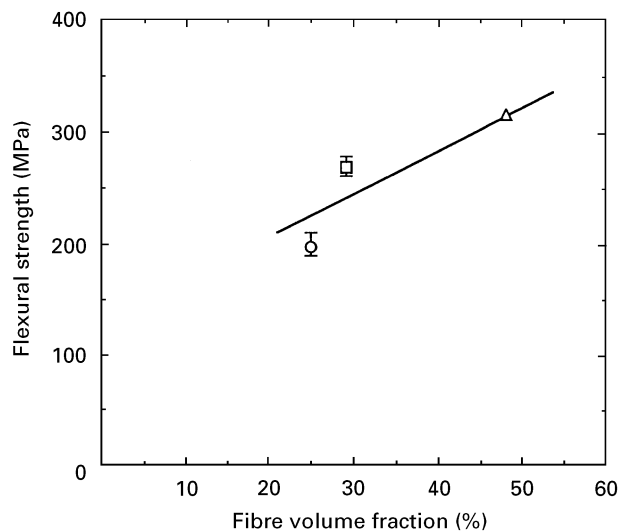


Figure 9 Dependence of flexural strength on fibre volume fraction; CVI temperature, 1373 K. (□), (○) and (△) correspond to flexural strength values of the A-type, B-type and C-type sample in  $L/d$  ratio range from 8.3 to 14.3 in Fig. 9, respectively.

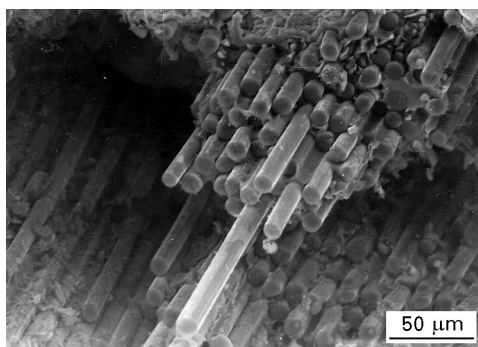
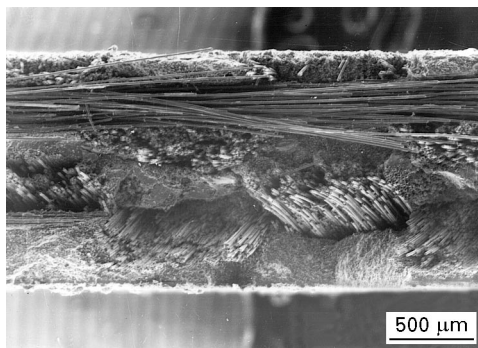


Figure 10 SEM images of the ruptured section of the sample after bending test; CVI temperature, 1373 K; number of pulses,  $7 \times 10^4$ ; preform, type-C;  $L/d$  ratio, 27.3.

prior to the bending rupture when the span length is short, and the flexural strength is estimated to be less than that for a long span. On the present sample, it is considered that the flexural strength is estimated to be low when  $L/d$  is below 8 (Fig. 8).

SEM images of the cross-section of the C-type sample after a bending test are shown in Fig. 10. Load is applied from the direction of the upper surface in the photograph. Pull-out of Tyranno fibres is observed, especially in the under surface layer of Tyranno cloth, in which the tensile force is applied when the sample is bent. This observation indicates the loose adhesion between the Tyranno fibre and the SiC matrix.

Fig. 11 shows the dependence of the ILSS of the sample obtained at 1373 K using B-type and C-type preforms on the number of pulses. ILSS increases with number of pulses in both types of samples. The ILSS of B-type and C-type samples reaches about 20 MPa at  $10 \times 10^4$  pulses and 40 MPa at  $7 \times 10^4$  pulses, respectively, and the ILSS of the C-type sample is about twice that of the B-type sample. These values are about 6 times higher than that of the original preforms. The volume fraction of SiC particles in the B-type sample is larger than that of the C-type sample (B-type, 45%; C-type 22%), therefore, the thickness of the layer of SiC particle in the B-type sample is higher

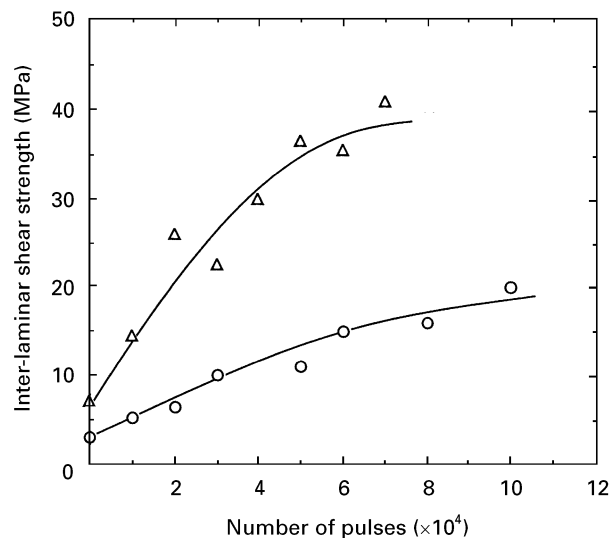


Figure 11 Dependence of inter-laminar shear strength on number of pulses; CVI temperature, 1373 K; preform, type-B (○) preform, type-C (△);  $L/d$  ratio, 4.

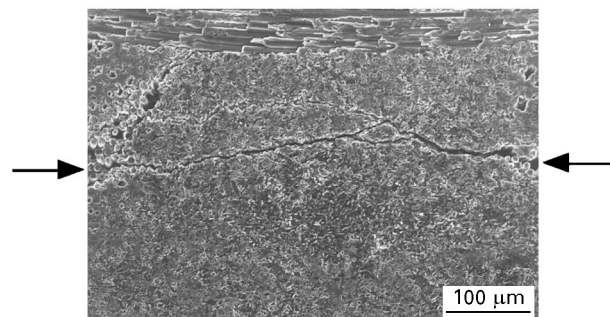
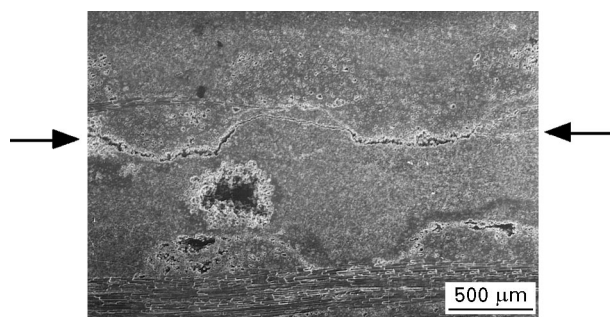


Figure 12 SEM images of the polished cross-section of the sample after inter-laminar shear strength test; CVI temperature, 1373 K; number of pulses,  $1 \times 10^5$ ; preform, type-B;  $L/d$  ratio, 4. Arrows indicate the fractures (cracks).

than that of the C-type sample. SEM images of the cross-section of the samples after a bending test are shown in Fig. 12. The cracks deflect and branch in the layer of SiC particles and/or along the interface of the layer of SiC particles and the Tyranno layer. It is considered that the layer of SiC particles between the Tyranno cloth layers enhances the adhesion of the two cloth layers as SiC is infiltrated and acts as a resistance to the inter-laminar shear fracture. In addition, when cracks propagate to SiC particles, cracks are deflected to the direction of the weaker SiC matrix. However, it is supposed that both flexural strength (Figs. 7 and 9) and ILSS (Fig. 11) may be weakened when the layer of SiC particles is too thick.

#### 4. Conclusion

Using a gas system of  $\text{SiCl}_4\text{-CH}_4\text{-H}_2$ , pressure-pulsed chemical vapour infiltration of SiC into 2D-Tyranno/SiC particulate preforms having different sizes and fibre volume fractions was investigated, and mechanical properties of infiltrated samples were evaluated. The following results were obtained.

1. The deposits obtained above 1373 K consisted of only  $\beta$ -SiC, whereas Si codeposition was found in the samples obtained at 1348 K.
2. At 1423 K, films on macrosurfaces were formed at an early stage. The most favourable temperature to obtain a high filling ratio of SiC into the preform without Si codeposition was considered to be 1373 K.
3. The SiC filling ratio of the sample obtained at 1373 K was 75%, which was equivalent to a residual porosity of 7.5%. The filling ratio was independent of the preform size.
4. The flexural strength increased with increasing filling ratio and fibre volume fraction in the sample. The flexural strength of the sample having 48% fibre volume fraction reached 290–340 MPa, after SiC was infiltrated above  $5 \times 10^4$  pulses at 1373 K.

5. Inter-laminar shear strength increased with number of pulses, and reached 40 MPa after  $7 \times 10^4$  pulses at 1373 K.

#### References

1. R. FEDOU, F. LANGLAIS and R. NASLAIN, in Proceedings of the Eleventh International Conference on CVD, edited by K. E. Shear and G. W. Cullen (Electrochemical Society, New Jersey, 1990) p. 513.
2. R. FEDOU, F. LANGLAIS and R. NASLAIN, *J. Mater. Synth. Process* **1** (1993) 61.
3. O. P. S. DUGNE, A. GUETTE, R. NASLAIN, R. FOURMEAU, Y. KHIN, J. SEVELY, J. P. ROCHER and J. COTTERET, *J. Mater. Sci.* **28** (1993) 3409.
4. T. M. BESMANN, R. A. LOWDEN, D. P. STINTON and T. L. STARR, *J. Phys. Coll. C5 suppl.* **5** (1989) p. C5-229.
5. T. M. BESMANN, R. A. LOWDEN, B. W. SHELDON and D. P. STINTON, in Proceedings of the Eleventh International Conference on CVD, edited by K. E. Spear and G. W. Cullen (Electrochemical Society, New Jersey, 1990) p. 482.
6. Y. G. ROMAN, D. P. STINTON and T. M. BESMANN, in Proceedings of the Eighth European Conference on CVD, edited by M. L. Hitchman and N. J. Archer (Les Editions de Physique, Paris, 1991) pp. C2–689.
7. K. SUGIYAMA and E. YAMAMOTO, *J. Mater. Sci.* **24** (1989) 3756.
8. K. SUGIYAMA and Y. OHZAWA, *ibid.* **25** (1990) 4511.
9. K. ITHO, M. IMUTA, A. SAKAI, J. GOTHO and K. SUGIYAMA, *ibid.* **27** (1992) 4070.
10. K. SUGIYAMA and K. YOSHIDA, *ibid.* **30** (1995) 5125.
11. P. DUPEL, R. PAILLER and F. LANGLAIS, *ibid.* **29** (1994) 1341.
12. P. DUPEL, R. PAILLER, X. BOURRAT and R. NASLAIN, *ibid.* **29** (1994) 1056.
13. J. YEHESEKEL and M. S. DARIEL, *J. Am. Ceram. Soc.* **78** (1995) 229.
14. K. SUGIYAMA and T. KISHIDA, *J. Mater. Sci.* **31** (1996) 3661.

Received 19 April 1996  
and accepted 11 February 1997